Establishing Programmable Josephson Voltage Standard and Maintaining Its Quantum Accuracy

Tezgül Coşkun Öztürk[1], Sarp Ertürk[2], Ali Tangel[2], Adem Gedik[1], Mesut Yoğun[1], and Murat Celep[1]
[1] TÜBİTAK Ulusal Metroloji Enstitüsü, P.K. 54, 41470, Gebze-Kocaeli, Turkey
[2] Kocaeli Üniversitesi, Müh Fak, Elektronik ve Haberleşme Müh, Umuttepe Yerleşkesi, 41380, İzmit-Kocaeli, Turkey
Email: {tezgul.ozturk; adem.gedik; mesut.yogun; murat.celep}@tubitak.gov.tr; {serturk; atangel}@kocaeli.edu.tr

***Abstract*—In this article, programmable Josephson voltage standard system established in TÜBİTAK UME is presented. The specifications of the instruments used in the system are defined and tested according to the needs of the system. Test setups are given in detail. The cryoprop used to immerse the superconducting integrated circuit into the liquid helium is manufactured. The horn antennas used in the waveguide part of the cryoprop are manufactured by employing wire erosion technique. The optical transceivers having low jitter for distributing trigger and clocks while keeping fully floating the system are manufactured. The software for generating quantum voltages and easy use of the system is prepared and equations used in the algorithm are given. The procedures to maintain the necessary accuracy of the bias electronics to maintain the quantum accuracy of the system is given in detail. The established system is used in metrological measurements and the results of the measurements which prove the quantum state of the system are presented.**

***Index Terms*—voltage, Josephson voltage standards, DAC, ADC static gain, dynamic gain**

I. Introduction

In 1962, Brain Josephson predicted the intrinsic behavior of the cooper pairs when they are tunneled through a thin barrier of insulator installed between two super conductors [1], and in 1963, his theory was proven [2], [3]. In the following years, many experiments [4] have been performed to prove the frequency voltage relation in which voltage and frequency are proportional by multiplication of physical constants and an integer. Several experiments have shown that the equation is independent from the geometry and material of the junction, power of the microwave and magnetic field [4]. The presence of such an equation promises the voltage agreement at the accuracy and stability of the frequency quantity.

The proof of this equation encouraged metrologists to measure 2e/h constant which is known as Josephson constant (KJ). The present value of KJ was accepted in 1990 and denoted by KJ-90 after a comparison which has 0.4 ppm uncertainty [5], [6]. Despite of this absolute uncertainty, accepting a conventional value for KJ-90 improved the voltage unity in the world firstly to 0.01 ppm level with single JJ and to 0.001 ppm level with arrays of JJs [7].

Connecting the JJs serially was possible in 1981 using underdamped JJs because of the lack of JJs with the same electrical attributes. With underdamped JJs, it is possible to generate VJ, while the dc current is zero for the all voltage steps, for n=0, ±1, ±2, ±3, ⋯ [8]. These DC zero current crossing voltage steps were enabling technology for Josephson voltage standards (JVS) and mostly called as conventional JVS while they had intrinsic and unwanted two disadvantages: 1) Changing rapidly between different steps was not possible and 2) noise sometimes could change the steps randomly [7].

In 1995, another kind of JVS having voltage steps, which are stable and programmable by changing the dc current, called as programmable JVS (PJVS), was suggested [7]. In this standard, JJs are over dumped and n is 0 or ±1. Different quantum voltages are selected by changing the dc current of the arrays of JJs divided into segments. This standard over comes the two disadvantages of the Conventional JVSs and moreover enables the dynamic measurements of DAC&ADCs at low frequencies. This technology was not possible in 1980s, but in 1995, this was possible because of the developments in junction manufacturing and on chip microwave power distributing technologies [7].

JVSs are the basis of electrical metrology [9], [10]. More than one PJVS system is necessary to disseminate quantum accuracy to electrical quantities. Instead of buying a ready system, TÜBİTAK UME preferred to establish its own system. This has the advantage of interchanging the parts of the system and establishing different setups using the PJVS systems.

In this study the established system is presented. The hints to keep the system at quantum state are addressed.

II. Components of the System

The heart of PJVS is the superconducting integrated circuit (SIC) consisting of over dumped JJs and distributed microwave architecture [11]. The Josephson voltage across one JJ is given in (1).

$$V_J = \frac{nfh}{2e} \tag{1}$$

Manuscript received January 15, 2018; revised March 1, 2018; accepted June 20, 2018.
Corresponding author: Tezgül Coşkun Öztürk (email: tezgul.ozturk @tubitak.gov.tr)

doi: 10.18178/ijeetc.8.1.19-25

where V_J is the voltage across the barrier when the super conducting Josephson Junction (JJ) is biased with appropriate dc and ac currents as illustrated in Fig. 1 [7]. f is the frequency of the AC current applied through the junction. h and e are the plank and the electron charge constants respectively and n is an integer.

The integrated circuit is borrowed from PTB within cooperation in Q-Wave and QuADC [12] projects. The integrated circuit has Nb as a super conductor. The temperature of superconductivity of Nb is 9.2 K. The temperature environment below 9.2 K is provided by liquid helium in a Dewar. A Dewar is a container which consists of nested cups with an outer layer of vacuum and liquid helium in the inner layer. The temperature at which the helium gas is fluidized is 4.2 K. The integrated circuit on a carrier shown in Fig. 2 is immersed in a liquid helium, via a so-called cryoprop.

The task of the cryoprop is to transmit microwaves and $\pm I_n$ currents shown in Fig. 1, as well as immersing the chip in liquid helium. The microwave source applies the high frequency AC signals shown in Fig. 1. The microwave power required at the antenna of the SIC for stable operation of the steps is around 50 mW. To lock the phase of the microwave source and thus to increase the frequency accuracy, a high-stability rubidium or cesium oscillator is used.

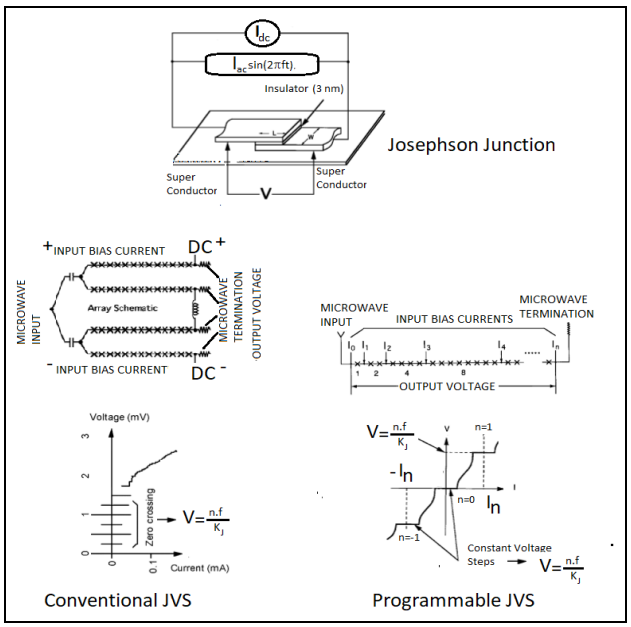

Fig. 1. Biasing Josephson junctions [7].

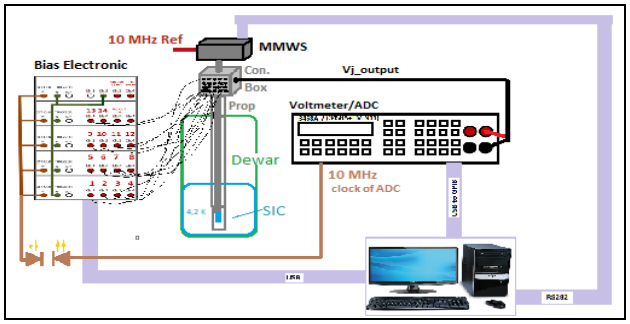

Fig. 2. Established PJVS system.

A magnetic shield is used to prevent the superconductivity from being affected by the external magnetic fields. The dc current illustrated in Fig. 1 is provided by the bias electronics. Each of the $\pm I_n$ currents shown in Fig. 1 is provided by DACs with voltage output that form the bias electronics.

The PJVS voltage needs to be "floating": For this reason, the synchronization signals must be converted to optical signals through the optical "transmitter" and then back to the electrical signal again via the optical "receiver". This process is carried out with an optical transceiver system.

In addition, the system consists of a 28-bit multimeter (voltmeter) that checks whether the generated voltage is in quantum step. Software on the computer calculates the DAC voltage and loads the voltage information into the DACs and receives the multimeter measurement data. The communication between the computer and the bias electronics and the multimeter uses optical hubs produced for long distance computer communication that helps to keep the quantum voltage floating. The system is shown in Fig. 2.

A. Cryoprop

The task of the cryoprobe is to transmit microwave and low frequency electrical signals to about 1 m between ambient temperature and superconducting temperature. The superconducting circuit operates at 68 GHz to 76 GHz. The "oversized" circular waveguide is used for microwave transmission at this frequency band (E band).

The 'Oversized' waveguide is a waveguide which has dimensions much larger than the wavelength. Such a waveguide attenuates the microwave much less compared to a rectangular waveguide. But the output of the microwave source and the element that couples the microwave to the chip is a rectangular waveguide at E band. An element called converter is a kind of horn antenna that provides a transition between a rectangular waveguide and a circular waveguide.

Converters are generally manufactured by electrolytically collecting copper on the mold. Since the converters cannot be produced in Turkey with this technology, the converters used in the system are produced by employing wire erosion technique. These converter parts are vital for prop construction. Non-magnetized, drawn steel tube is used for the waveguide. Fig. 3 shows the waveguide in the probe.

The insulator shown in Fig. 3 is manufactured to prevent ground loops by placing a thin Teflon plate between two of the 1-inch rectangular waveguides with Teflon screws.

Fig. 4 shows the measurements of attenuation obtained using the microwave source (millimeter wave synthesizer--MMWS) and the maximum microwave power delivered to the probe when using the manufactured probe and the purchased microwave source.

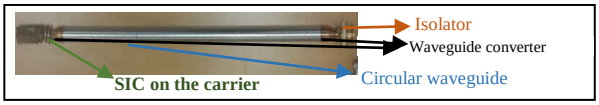

Fig. 3. Waveguide part of the prop.

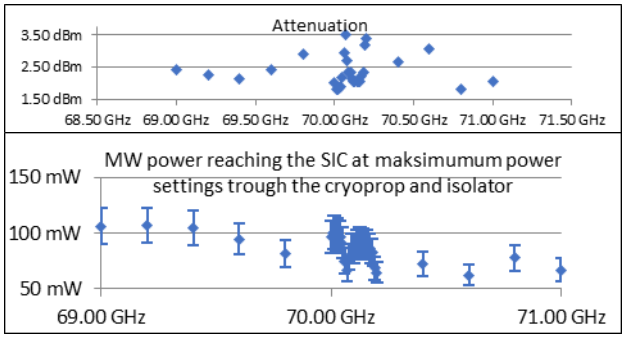

Fig. 4. Attenuation measurements of the cryorop.

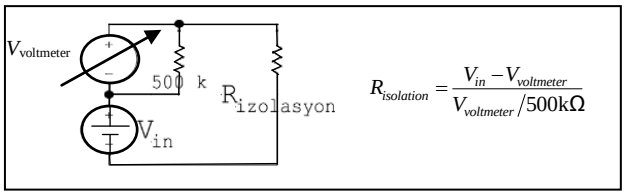

Fig. 5. Insulation resistance measurements of the prop.

These measurements show that the system consisting of the cryoprop and microwave sources is suitable for operating the superconducting integrated circuit. The microwave power absorbed by the probe also varies with the prop's temperature distribution. The temperature distribution throughout the prop varies with the change in liquid helium level.

The low frequency currents (bias currents) of the multi arrays of JJs over the prop are conducted with twisted two-wire transmission lines to reduce inductive effects. A wire with insulation material even when twisted is unbreakable was searched. Insulation resistance of the transmission line was measured using the setup given in Fig. 5. Measurement results have shown that wire manufactured according to the IEC60317-51 standard is suitable.

It is ensured by measuring that the insulation resistance between the two wires of a channel, between the channels, between the channels and the probe, and between the output voltage lines is greater than 500 GΩ. The internal resistance of the voltmeter given in Fig. 5 is higher than 10 MΩ and the voltmeter is operated by a battery. The V_{in} voltage was selected to be 500 V so as not to exceed the maximum rated voltage given in IEC60317-51. Teflon insulated SMB connectors, one for each channel are used on the prop to couple the bias currents. The reason for choosing these connectors is that they can easily be plugged and unplugged and the frequency bandwidths are on the order of 4 GHz. The benefit of this structure is that each array of JJs can be biased separately. Two-wire transmission lines are planned to transmit signals with frequencies less than 40 kHz.

B. Microwave Source

Microwave source is used to apply the high frequency AC current which are illustrated in Fig. 1 to the JJs. Two different MMWS are tested and used. The necessary specifications and the reason of this specifications for the MMWS are given in [13]. Fig. 6 is the measurement setup where the microwave power and the frequency of the MMWSs are tested simultaneously. The stability and accuracy of the Josephson voltage steps depend on the frequency of the microwave as in (1). The quantity produced with the lowest uncertainty is time. When an oscillator is generated by rubidium/cesium clocks the long and short-term stabilities are relatively more stable than 10^{-10} to 10^{-14} orders. For this reason, the millimeter wave synthesizer is locked into the phase of the external 10 MHz rubidium/cesium oscillator to produce the frequency of the microwave within this stability. The frequency stability, while it is locked to the external clock, is less than ±5 Hz when measured with EIP counter (the instrument is given only to completely define the measurement setup and using the instrument is not an advice or obligation) as shown in Fig. 6. Measurement results obtained with the setup given in Fig. 6 are summarized in the graphs given in Fig. 7. Microwave (MW) Power for power settings covering the all settable range is measured dependent on many frequencies, and flatness at the settings is also investigated for the two used MMWS.

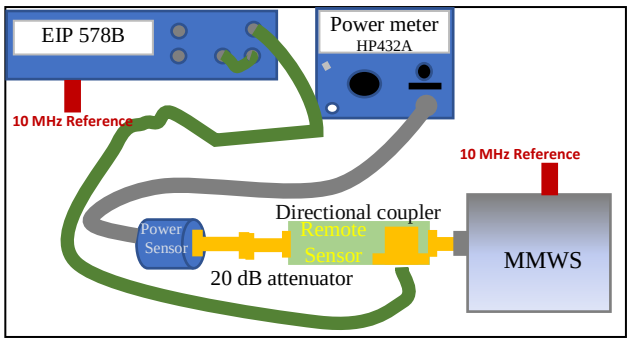

Fig. 6. Measurement setup of MMWS1.

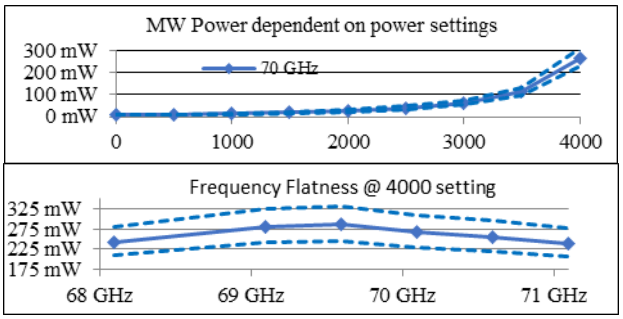

Fig. 7. Measurement results of MMWS.

C. Bias Electronics

Arbitrary waveform generators (AWG) consisting of 4 channels of DACs, which are previously used for this purpose in [14] are selected. Using a synchronization cable up to 8 of these generators can be synchronized and act as a 32-channel generator. With this synchronization cable, the low potential of each DAC which provide the $\pm I_n$ currents shown in Fig. 1 is shorted. There are two different connection schemes that can be used for supplying bias currents: One is by short-circuiting the low-potential ends of each channel to the low-potential end of the array, and the other one is by connecting each DAC in series. The DACs purchased in this study are not isolated and when synchronized, they are hardware-connected as shown in Fig. 8 and in [15].

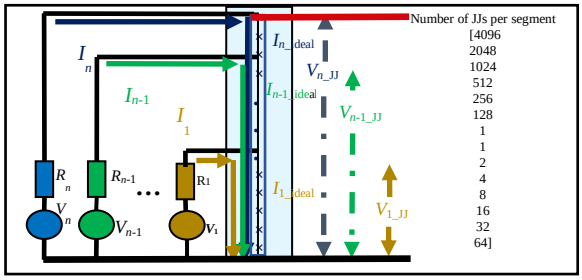

Fig. 8. Connection diagram of DACs & arrays of JJs.

There are 14 independent JJs segments in the SIC used. The DACs can generate signals of any shape simultaneously using each channel's dedicated memories. Each channel can supply 12 $V_{pk\text{-}pk}$ at 50 Ω load. DACs can produce at least at 16-bit resolution with a sampling rate of at least 1 GS/s for each channel. Channels can be operated synchronously with each other and be triggered by an external trigger signal. The synchronization (delay) between channels are measured to be less than 3 ns using Agilent 86100B with 50 GHz Module sampling oscilloscope. The memory of each channel can be accessed independently. The software control of the DACs is provided by an optically isolated PC as shown in Fig. 2.

D. Optical Transceiver System

The heart of the optical converters is 820 nm wavelength sensors from Avago. These sensors have been developed for industrial and communication applications at speeds of up to 32 MBd [16]. The PCBs of the transceivers, as seen in Fig. 9, have been manufactured by a local company with electronic components and circuit diagram provided. The transducers are mounted in aluminum boxes as shown in Fig. 9. The isolation between the boxes and the transceivers is greater than 500 GΩ. This level of isolation is achieved by using isolated BNC connectors.

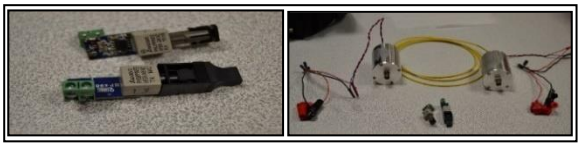

Fig. 9. Optical transceiver system.

The stability of the timing signal is important, and the jitter parameter of the produced transducers is investigated. An accurate jitter measurement is made using the SR620 counter (The instruments are given only to completely define the measurement setup and using these instruments is not an advice or obligation). The 1 kHz signal generated by the counter is applied to the two channels of this counter with equal length of cables. The standard deviation of the delay between the two channels is the jitter caused by the cable and the circuits of the counter. The jitter from the counter's own circuitry ($t_{j\_counter}$) is measured less than 15 ps. Then a 1 kHz signal from one of the channels is applied by passing through the transceiver system as shown in Fig. 10. In this case, the jitter ($t_{j\_measured}$) is measured as 150ps. Using (2), the jitter of the transceiver system ($t_{j\_transceiver}$) is determined to be approximately 149ps.

$$t_{j\_measured} = \sqrt{t_{j\_counter}^2 + t_{j\_transceiver}^2} \quad (2)$$

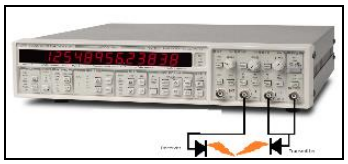

Fig. 10. Jitter Measurement Setup.

III. Programming the Bias Electronics for Generating Quantum Voltages

A. DAC Calibration

Each DAC in each channel has 16-bit resolution and in serial 50 Ω resistor inside, which means around 20 μA current resolution. The accuracy of the DAC outputs is specified by the manufacturer as '0.25% of range'. With 12 V measurement range, this accuracy corresponds to 30 mV resulting to 600 μA. With repeated calibration of DACs, it is measured that the stability of DAC offsets is less than 500 μV, and the DAC's gain stability is much better than 300 ppm during a few weeks. In this way, the current stability for the worst case is ~ 80 μA and it can be set more precisely than 600 μA by calibration. In other words, the calibration of DACs is important, and it is vital especially for the arrays where the critical current is small. In addition to the output voltage, the output resistance of the DAC is measured. The stability of the output resistance is less than 500 μΩ/Ω which means that the contribution of instability due to resistance when the dc current shown in Fig. 1 is 10 mA, is 5 μA which is much less than the current resolution of the bias electronics. For the calibration of the DACs, a software that automatically performs the following operations is prepared using the measurement setup given in Fig. 11.

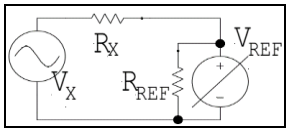

Fig. 11. DAC Calibration Circuit.

1) An external R_{REF} (1 kΩ or 50 Ω) is calibrated with the multimeter,

2) The following are repeated for each channel in turn:

2a) The output of the DAC is set to a ramp of 10-20 points to cover the entire application range. V_x voltages are measured when R_{REF} is not connected. In this case, the input impedance of the voltmeter is above 10 GΩ and the loading effect of R_x resistor at the output of the DAC is negligible.

Taking the advantage of the equation $V_x = V_{REF}$, the gain and offset of the DAC are determined ($V_x = mV_{set} + n$). V_{set} is the voltage to which the DAC output is set. m is gain and n is offset of the DAC.

2b) R_{REF} is connected to the input of the voltmeter. The measurements in step 2a) is repeated and recorded as V_{R_REF}.

2c) The R_X for each point is measured using these two measurements and is derived by (3). The V_x term in (3) is determined using the formula ($mV_{set}+n$), taking advantage of m and n measured in step 2a).

TABLE I. EXAMPLE TABLE FOR DAC CALIBRATION AND STABILITY ANALYSIS

Channel	m+ [V/V]	n+ [V]	R_x [Ω]	m-[V/V]	n-[V/V]	$(m-\bar{m}^+)/\bar{m}^+$	$n^+-\bar{n}^+$	$(R_X-\bar{R}_X)/\bar{R}_X$	$(m^--\bar{m}^-)/\bar{m}^-$	$(n^--\bar{n}^-)/\bar{n}^-$
0	0,99910	0,00024	50,7819	0,99934	0,00150	−12 ppm	76 µV	<500 µΩ/Ω	−11 ppm	86 µV

2d) The DAC's gain, offset and output resistance are recorded in the excel file along with the DAC serial number and channel number. This file is automatically called by the software that programs the DACs for quantum voltage generation. For each channel, the output results are analyzed as given in Table I.

The positive and negative offset of the DACs are not equal. For this reason, separate gains (m) and offsets (n) are calculated for positive and negative values. In addition to offsets, gains of positive and negative polarity are also different.

$$V_x \frac{R_{\text{REF}}}{R_{\text{REF}}+R_X} = V_{R\_\text{REF}} \tag{3}$$

B. Measuring the Margins of the Setup

Fig. 8 shows the SIC and bias electronics connection. The I_{n_ideal} currents shown in this figure correspond to the currents $\pm I_n$ shown in Fig. 1. In other words, the I_{n_ideal} currents are the midpoints of the current widths of the 0^{th} and $\pm 1^{\text{st}}$ Shapiro steps [3]. This width is called as margins. These points are measured by independently biasing each segment of junctions in the whole circuit and measuring the midpoints of current margins.

The bias margins depend on the frequency of the microwave and the microwave power reaching the chip. The microwave power reaching the chip changes with the level of liquid helium. As a result of a significant reduction in the helium level, the I_{n_ideal} measurements are repeated. Trap flux is a common problem in PJVS systems and the chip needs to be heated to get rid of this problem. Heating can be done by removing up and then dipping the probe, or it can be done with a heater resistor placed just behind the chip. If the heating process is carried out with heater resistance, the helium level changes less and once measured I_{n_ideal} currents are applied for a much longer time. The operation of the system at (I_{n_ideal}) currents is important because it does not deviate from the quantum voltage due to the instabilities of the bias electronics, also the effect of transients is small [17].

The critical current (I_c) is measured after liquid helium submersion of the SIC. If the critical current is equal or close to the theoretical value, it indicates that there is no trapped flux on the integrated circuit.

In order to find the optimum combination of microwave frequency and power, a sinewave with 4 samples at maximum amplitude is generated with all JJs and the *I-V* curve is drawn by biasing the whole array with only one channel and iterating the estimated I_{n_ideal} currents up to $\pm I_c/2$. *I-V* curves are measured for many microwave power and frequency settings by performing frequency and microwave power iterations under software control. The $\pm 1^{\text{st}}$ Shapiro and 0^{th} Shapiro step widths measured under software control are both recorded in an excel file and graphically plotted. Frequency and microwave power pair which has more than 1 mA 0^{th} Shapiro width, and the wider nearly 2 mA $\pm 1^{\text{st}}$ Shapiro width, and which are not changing with adjacent frequencies are selected as optimum for the chip with 6 mA critical current. After finding the optimum power and frequency, I_{n_ideal} currents are measured as follows under this MMWS settings: For channels except the 1^{st} channel, the Josephson DAC is configured for n channels, but only two channels (I_n and $I_{n\text{-}1}$) are connected. This means that only the most significant two DACs belonging to the channels are connected and used for measurements. For the selected channel (n), the amplitude of the quantum voltage is set again to 4 sampled sine wave such that the n^{th} segment is $\pm 1^{\text{st}}$ an 0^{th} Shapiro step, and the rest segments are always on 0^{th} Shapiro step. In this way, the *I-V* curve of each segment of JJs is obtained and the I_{n_ideal} currents are measured as in Fig.12. The segment including only one junction, seen in red color has very small margins which is not acceptable to be used at $\pm 1^{\text{st}}$ Shapiro steps.

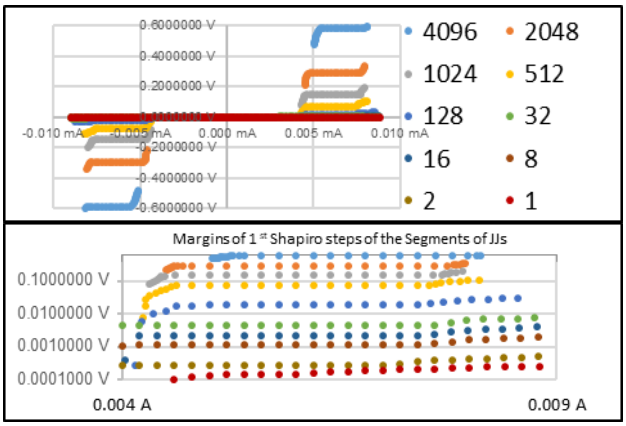

Fig. 12. Measurement of I_{n_ideal} currents.

The currents in the *I-V* curve measurements shown in Fig. 12 are calculated by the software by employing the equation (4). In (4) the n^{th} DAC channel settled voltage is V_n, measured voltage using the voltmeter shown in Fig. 2 is V_{quantum} and resistance R_n is the sum of the output resistance of the DAC and cable resistance. I_{n_ideal} currents found in this way are recorded in a text file and are automatically called by the software which is programming the DACs for quantum wave generation.

$$I_n = \frac{V_n - V_{\text{quantum}}}{R_n} \tag{4}$$

C. Programming the Bias Electronics

In Fig. 8, each DAC is shown in a different color, and the currents delivered from corresponding DACs are marked with the same color with the DACs. The quantum voltage seen from each channel is also marked with the same color with the DAC. In Fig.8, the most significant n^{th} channel's current is given by (5).

$$I_n = I_{n\_\text{ideal}} \tag{5}$$

$$I_{n-1\_ideal} = I_{n\_ideal} + I_{n-1};\ \ I_{n-1} = I_{n-1\_ideal} - I_{n\_ideal} \quad (6)$$

By using (6), each DAC's current is calculated. For example, if each JJs is programmed in the +1st Shapiro and If I_{n_ideal} = 7 mA and $I_{n\text{-}1\_ideal}$ = 7.2 mA are measured, then $I_{n\text{-}1}$ should be $I_{n\text{-}1}$ = 0.2 mA. After calculating each DACs current, each DAC voltage is calculated using the (7). V_{n_JJ} in (7) is the Josephson Voltage seen from the n^{th} DAC. Satisfying (7) guaranties DAC currents to flow as shown in Fig. 8.

$$V_n = I_n R_n + V_{n\_JJ} \quad (7)$$

With the first 4 AWG generators, 14 independent DACs are used to bias the 14 independent segments as shown in Fig. 8 to the appropriate Shapiro step. The trigger signal per period is generated from 15th channel. In the 16th channel, a trigger signal per measurement is generated. To generate arbitrary quantized waves, DACs are programmed as follows:

1) Arbitrary wave parameters to be generated: wave shape, amplitude, step number are selected via the interface program.

2) Each step is quantized by the quantization algorithm.

3) For each quantum step, the voltages of the 14 DACs are calculated using (5) - (7). The voltages of each DAC are stored in arrays and are recorded in files with the channel's name.

4) This process is repeated for each quantum step in sequence.

5) Recorded voltages are corrected using the generated calibration file recorded as in Table I. Corrected DAC voltages are recorded to each independent DAC's memory of the generators as a 4-step DC wave.

At each external trigger pulse, the DAC voltages are triggered to the next quantum voltage. The trigger signal is generated by an additional 5th AWG generator. The frequency of the trigger signal is equal to the frequency of the signal multiplied by the number of steps. In addition, timing signals are produced at frequencies of 20 MHz and 10 MHz from the 5th generator.

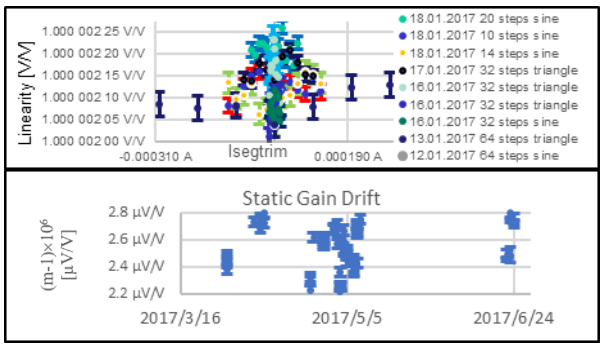

Fig. 13. Static linearity measurement results.

IV. Metrological Measurements

A. Static ADC Characterization

Whether the voltage output is at quantum level for all codes/steps can be controlled quickly by using the voltmeter in the system. The ADC is also statically characterized by evaluating the results of this control. Fig. 13 is a result of this static calibration. The measured stability of the gain is much less than 0.5 ppm which is previously declared in [18] and it is obvious that the gain of the ADC is independent from $I_{segtrim}$ that indicates the quantum state.

B. Solid State Voltage Standard (SSVS) Calibration

SSVSs are traceable to the Conventional JVSs. Rather than directly comparing the JVSs, to use the SSVS as a transfer standard has been preferred in terms of the simplicity and the cost of measurement. Established PJVS system is compared with the SSVS. Measurement results are summarized in Fig.14. Measurement results show that the result is independent from $I_{segtrim}$ and the two results are agreed within the stability of SSVS.

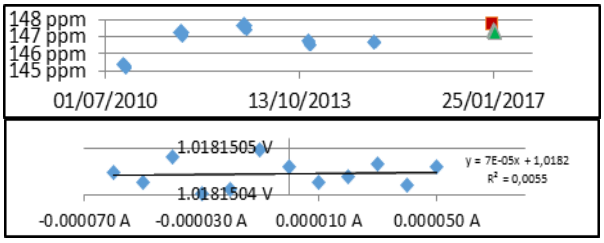

Fig. 14. History and measurement results of the SSVS

C. Dynamic ADC Characterization

Dynamic ADC Characterization is explained in more detail in [18], the PJVS standard is used to investigate how ADC gain changes depending on the dynamic conditions. For this measurement, the ADC is modified to take out its timing signal using developed optical transceiver system. This timing signal is applied to the bias electronics as seen in Fig. 2, which is important to obtain measurements at the center of the quantum steps. In Fig. 15, the obtained measurement results are summarized.

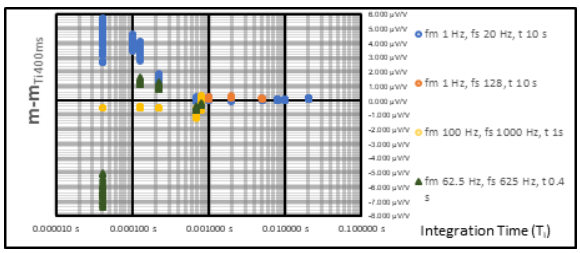

Fig. 15. Dynamic ADC characterization.

V. Conclusions

In this article, Programmable Josephson Voltage Standard system established in UME was presented. Every part of the system was bought/manufactured separately and tested according to the needs of the system. The necessary measurements of microwave, cryoprop, optical transceivers and bias electronics to maintain the quantum accuracy of the output voltage are given in detail. The hints of the software for generating quantum voltages and easy use of the system were described. The system was used in static and dynamic ADC characterization and SSVS calibration. Measurement results has shown that the system was established

successfully. A detailed procedure about the measurements and uncertainty evaluation were presented in [19].

ACKNOWLEDGEMENT

This work is partly carried out with funding by the European Union within the EMRP Q-WAVE and EMPIR QuADC projects. The EMPIR initiative is so co-funded by the European Union's Horizon 2020 research and innovation program and the EMPIR Participating States. T.C.Ö. wants to thank Ralf Behr and Johannes Kohlmann for valuable discussions on Josephson Voltage Standard Systems and PTB for borrowing the SIC. T.C.Ö. also wants to thank to Menar Electronics for their cooperation in PCB manufacturing of the optical transceivers and Gülmak Tor.Tes.San.Pls.İml.Ltd.Şti. for waveguide converters (horn antennas) manufacturing. T.C.Ö. also wants to thank to Saliha Turhan for her support on waveguide manufacturing and Mehedin Arifoviç for his resource leading within the laboratory.

REFERENCES

[1] B. D. Josephson, "Possible new effects in superconductive tunneling," *Phys. Letters*, vol. 1, no. 7, pp. 251-253, 1962.

[2] P. Anderson and J. M. Rowell, "Probable observation of the Josephson superconducting effect," *Phys. Rev. Lett.*, vol. 10, no. 6, pp. 230-232, 1963.

[3] S. Shapiro, "Josephson currents in superconducting tunneling: The effect of microwaves and other observations," *Phys. Letters*, vol. 11, no. 2, pp. 80-82, July, 1963.

[4] P Pöpel and R., "The Josephson effect and voltage standards," *Metrologia*, vol. 29, no. 2, pp. 153-174, 1992.

[5] V. Sienknecht and T. Funck, "Realization of the SI unit volt by means of a voltage balance," *Metrologia*, vol. 22, no. 3, pp. 209-212, 1986.

[6] B. N. Taylor and T. J. Witt, "New international electrical reference standards based on the Josephson and quantum hall effects," *Metrologia*, vol. 26, no. 1, pp. 47-62, 1989

[7] S. P. Benz and C. A. Hamilton, "Application of the Josephson effect to voltage metrology," *Proc. of the IEEE*, vol. 92, no. 10, pp. 1617-1629, 2004.

[8] R. L. Kautz, "On a proposed Josephson effect voltage standard at zero current bias," *Appl. Phys. Lett*., vol. 36, no. 5, pp. 386-388, 1980.

[9] R. Behr, O. Kieler, J. Kohlmann, F. Müller, and L. Palafox, "Development and metrological applications of Josephson arrays at PTB," *Meas. Sci. Technol*., vol. 23, no. 12, 2012.

[10] J. Lee, R. Behr, B. Schumacher, L. Palafox, M. Starkloff, A. C. Böck, and P. M. Fleischmann, "From AC quantum voltmeter to quantum calibrator," presented at Conf. on Precision Electromagnetic Measurements, Ottawa Canada, 10-15 July, 2016.

[11] F. Mueller, R. Behr, T. Weimann, L. Palafox, D. Olaya, P. D. Dresselhaus, and S. P. Benz, "1 V and 10 V SNS programmable voltage standards for 70 GHz," *IEEE Trans. Appl. Supercond*., vol. 19, no. 3, pp. 981-986, Jun. 2009.

[12] EMPIR (2015). QuADC: Waveform metrology based on spectrally pure Josephson voltages. [Online]. Available: https://www.ptb.de/empir/quadc-project.html

[13] İ. Ünal, M. Tekbaş, A. Kaya, T. Coşkun Öztürk, "Millimeter wave synthesizer for Josephson voltage standard system," presented at Elektrik Elektronik ve Biyomedikal Müh. Konferansı, Bursa, Turkey, December 1-3, 2016.

[14] M. Schubert, M. Starkloff, J. Lee, R. Behr, L. Palafox, A. Wintermeier, A. C. Böeck, P. M. Fleischmann, and T. May "An AC Josephson voltage standard up to kilohertz range tested in a calibration laboratory," *IEEE Trans. Instr. Meas*., vol. 64, no. 6, pp. 1620-1626, 2015.

[15] J. M. Williams, D. Henderson, P. Patel, R. Behr, and L. Palafox, "Achieving sub-100-ns switching of programmable Josephson arrays," *IEEE Trans. Instr. Meas*., vol. 56, no. 2, pp. 651–654, 2007.

[16] A. Technologies. Inexpensive dc to 32 MBd fiberoptic solutions for industrial, medical, telecom, and proprietary data communication applications. [Online]. Available: ttps://media. digikey.com/pdf/data%20sheets/avago%20pdfs/fiberoptic_solutions_appnote.pdf

[17] J. Lee, R. Behr, A. S. Katkov, and L. Palafox, "Modeling and measuring error contributions in stepwise synthesized Josephson sine waves," *IEEE Trans. Inst. Meas*., vol. 58, no. 4, pp. 803–808, 2009.

[18] K. W. G. Ihlenfeld, *Maintenance and Traceability of AC Voltages by Synchronous Digital Synthesis and Sampling*, Braunschweig, Germany: PTB Report E-75, 2001.

[19] T. C. Öztürk, S. Ertürk, A. Tangel, S. Turhan, and M. Arifoviç, "Metrological measurements using programmable Josephson voltage standard," presented at 10th Int. Conf. on Electrical and Electronics Engineering, Bursa, Turkey, November 30- December 2, 2017.